

## Application of the generalized-gradient approximation to rare-gas dimers

David C. Patton and Mark R. Pederson

*Complex Systems Theory Branch, Naval Research Laboratory, Washington, DC 20375*

(Received 10 April 1997)

By performing numerically precise calculations on the  $\text{He}_2$ ,  $\text{Ne}_2$ ,  $\text{Ar}_2$ ,  $\text{Kr}_2$ ,  $\text{HeNe}$ ,  $\text{HeAr}$ ,  $\text{HeKr}$ ,  $\text{NeAr}$ ,  $\text{NeKr}$ , and  $\text{ArKr}$  diatomic molecules we have determined the capacity of three popular approximations to density-functional theory to accurately describe bonding in these rare-gas systems. The local-density approximation, the Perdew-Wang 1991 generalized-gradient approximation, and the Perdew-Burke-Ernzerhof generalized-gradient approximation are utilized in the calculation of equilibrium bond lengths, atomization energies, and anharmonic and harmonic vibrational frequencies. We also use the density-functional-based determination of atomic polarizabilities and ionization potentials to obtain the coefficients for the long-range ( $1/r^6$ ) attraction. Our calculations suggest that the interaction from the overlap of atomic densities is the primary binding mechanism in these systems at short range but that the long-range  $1/r^6$  attraction could also contribute to the total binding energy. [S1050-2947(97)51009-2]

PACS number(s): 31.15.Ew, 03.65.Db, 31.10.+z

The debate as to whether approximations to the density-functional theory should describe bonding between closed-shell systems is long standing. While it is clear that no mean-field treatments are capable of reproducing the long-range fluctuating dipole ( $1/r^6$ ) attraction between two closed-shell systems, it is not immediately obvious whether a specific mean-field approximation may include other short-range attractions that could cause a binding between two closed-shell systems. One of the earliest attempts to describe bonding between noble-gas dimers within a density-functional approximation was a Thomas-Fermi treatment by Gordon and Kim [1]. In that work they assumed that at close distances the bonding between rare-gas dimers was dominated by the overlap of atomic densities and not by long-range  $1/r^6$  dispersion forces. By using a Thomas-Fermi kinetic-energy functional and a Kohn-Sham-Dirac exchange functional it was shown that a weak binding exists and that the results were in semiquantitative agreement with experiment. Many refinements and extensions to this method have been suggested and a good review of them has been given by Parr and Yang [2].

The kinetic-energy repulsion associated with a Kohn-Sham framework [3] is certainly different from that obtained by the Thomas-Fermi kinetic energy, and there is not currently a consensus on whether existing Kohn-Sham formulations of density-functional theory should be capable of describing bonding between two closed-shell systems. Early work by Worth *et al.* showed that the  $X\alpha$  method leads to an overbinding in  $\text{Ne}_2$  [4]. More recently Lacks and Gordon [5] have studied binding in  $\text{He}_2$  and  $\text{Ne}_2$ . They limited their study to the binding due solely to the exchange energy. They reported that the Perdew-Wang 1986 (PW86) [6] exchange functional was more accurate than the local-density approximation (LDA), Becke86A, Becke86B, Becke88 [7], DK87 [8], and PW91 [9] exchange functionals. Most recently, Perez-Jorda and Becke [10] have studied six rare-gas dimers within the LDA; the “half-and-half” functional of Becke [11]; the generalized-gradient-approximation (GGA)-exact-exchange mixture of Becke [12]; and a GGA functional composed of the Perdew and Wang LDA [13], the gradient-dependent exchange correction of Becke [7], and Perdew’s

gradient correction for correlation [9]. They found that the LDA severely overestimates the dissociation energies and the “half-and-half” functional tends to underestimate the binding. Their GGA calculations were not done self-consistently and gave repulsive potential-energy curves devoid of minima. Very recently in a paper aimed at benchmarking the PBE GGA functional on many different molecules, Patton *et al.* presented density-functional-based results on the  $\text{Ar}_2$  and  $\text{Ne}_2$  dimers that showed that these two molecules were reasonably well described by the GGA [14]. Finally Dobson and Dinte have developed a density-functional theory that allows for the derivation of the long-range  $1/r^6$  interaction between two *nonoverlapping* many-electron systems [15].

The purpose of this paper is to more carefully analyze the description of rare-gas dimers within traditional implementations of density-functional approximations and determine the relative merits of several of these approximations for the calculation of these low-energy interactions. In addition to studying the short-range attractions within density-functional approximations, we utilize the more simple approximations [16] to estimate the effects due to the long-range  $1/r^6$  attractions.

In this paper we present results for the same set of molecules, as studied by Perez-Jorda and Becke, plus four additional rare-gas dimers that involve krypton. We have utilized the LDA-PW91 [13], GGA-PW91 [9], and GGA-PBE [17] functionals in this work. We present energies, equilibrium bondlengths, and vibrational frequencies that are converged with respect to basis-set and numerical precision. All possible sources of errors (e.g., mesh and basis-set superposition errors) are accounted for here. In addition to presenting results that employ large basis sets, we have also performed calculations with minimal basis sets. A comparison between the latter and former numerical results provides information about what causes the short-range binding between these rare-gas systems.

Next we will give a description of the computational methods utilized in this study. This is followed by the results of calculations of atomization energies, equilibrium bond lengths, and vibrational frequencies. We then conclude with

TABLE I. Binding energies in eV for ten noble-gas diatomic molecules as calculated within the PW91 LDA, the PW91 GGA, and the PBE GGA. At the bottom of the table are listed in eV the average error ( $\delta$ ) and rms error for each of the approximations. Exact values are from Ogilvie and Wang [22].

Molecule	Exact	LDA	GGA-PW91	GGA-PBE
He <sub>2</sub>	0.0009	0.0094	0.0103	0.0032
Ne <sub>2</sub>	0.0036	0.0199	0.0143	0.0056
Ar <sub>2</sub>	0.0123	0.0289	0.0142	0.0061
Kr <sub>2</sub>	0.0173	0.0335	0.0143	0.0066
HeNe	0.0018	0.0147	0.0123	0.0043
HeAr	0.0025	0.0142	0.0114	0.0039
HeKr	0.0025	0.0138	0.0111	0.0038
NeAr	0.0058	0.0231	0.0144	0.0058
NeKr	0.0061	0.0240	0.0145	0.0060
ArKr	0.0156	0.0308	0.0142	0.0062
$\delta$		0.0144	0.0063	-0.0017
rms		0.0147	0.0079	0.0051

a discussion of the results and an analysis of possible contributions to the binding energy by van der Waals interactions.

The density-functional calculations performed in this study were done with the all-electron self-consistent cluster codes of Pederson and Jackson [18,19]. The codes combine large Gaussian-orbital basis sets, numerically precise variational integration techniques, group theory, and the analytic solution of Poisson's equation to accurately determine the self-consistent-field (SCF) potentials, secular matrix, total energies, and Hellmann-Feynman-Pulay forces. Since an important goal of this study is to ascertain the difference between the three approximations to density-functional theory (DFT) for rare-gas dimers and since the energy scale is so small, special care has been taken to produce fully converged results devoid of uncertainties due to basis sets and numerical precision. For each atom we used a contracted Gaussian-orbital basis set that would exactly reproduce the atomic total energies that would be obtained from a basis set of single Gaussians. The exponents for the single Gaussians have been fully optimized for the density-functional calculations [20]. The helium basis set is then constructed by contracting these eight bare Gaussians to form the atomic  $1s$  orbital. In addition, three  $s$ -type single Gaussians (using the three longest-range bare Gaussians), three  $p$ -type single Gaussians (using the fifth, sixth, and seventh bare Gaussians listed above), and one  $d$ -type single Gaussian (using the sixth bare Gaussian) complete the basis set for helium. For neon there are 14 even tempered bare Gaussians used to construct the atomic  $1s$ ,  $2s$ , and  $2p$  orbitals. In addition three  $s$ -type, three  $p$ -type, and three  $d$ -type single Gaussians are added to the neon basis set. For argon there are 17 even tempered bare Gaussians used to construct the atomic  $1s$ ,  $2s$ ,  $3s$ ,  $2p$ , and  $3p$  orbitals. In addition three  $s$ -type, three  $p$ -type, and three  $d$ -type single Gaussians are added to the argon basis set. For krypton there are 21 even tempered bare Gaussians used to construct the atomic  $1s$ ,  $2s$ ,  $3s$ ,  $4s$ ,  $2p$ ,  $3p$ ,  $4p$  and  $3d$ , orbitals. In addition three  $s$ -type, three  $p$ -type, and three  $d$ -type single Gaussians are added to the krypton basis set. The Gaussian exponents used for the basis sets are available upon request.

Since we are studying systems that are very weakly bound, it is important to make sure that the binding is not due to any basis-set superposition error (BSSE) [21]. The calculation of BSSE is straightforward with our codes. After

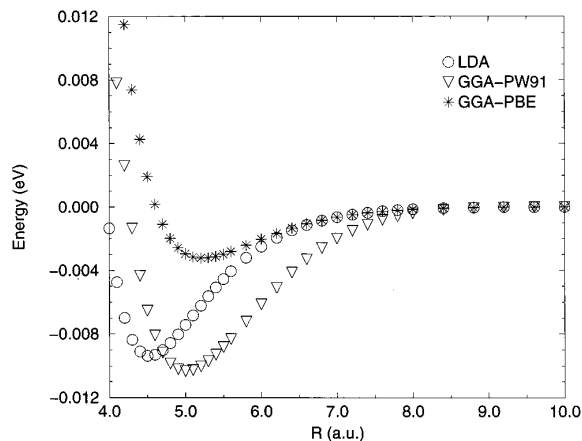


FIG. 1. He<sub>2</sub> binding-energy curves for LDA, GGA-PW91, and GGA-PBE.

self-consistently converging on the kinetic energy for a particular geometry of a diatomic molecule, we then utilize the same mesh and basis set for the calculation of an atom whose position coincides with one of the atoms of the diatomic molecule. In principle, the atomic reference energies can change due to two effects. First, since the atomic reference energy is calculated with a more complete basis, the variational principle states that the atomic reference energy could decrease slightly. Second, since the meshes used for the dimer calculations are different from those used for a spherically symmetric atom, there can be slight numerical differences that are not variational. As discussed below the basis-set superposition error is small and the “mesh superposition” error vanishes by virtue of high numerical precision.

The numerical precision of the SCF potentials and energies is maximized by using an analytic solution of Poisson's equation. All numerical integrations are performed on an efficient mesh generated via a variational technique and are accurate enough to integrate the total charge and the kinetic energy to ten-decimal-place accuracy. The variational mesh generation technique has been described in detail by Pederson and Jackson [19]. A key feature of the technique is the partitioning of space into atomic spheres, excluded cubic regions, and interstitial parallelepipeds, and then determining integration meshes for each region. We used the following parameters for the mesh in these regions: inside the atomic spheres the angular integrands utilized polynomials up to degree 21 and the radial integrands were converged to one part in  $10^{12}$ ; in the excluded cubic region we used 1920 angular points and radial integrations converged to one part in  $10^{12}$ ; in the interstitial parallelepipeds each of the three one-dimensional test integrals was converged to one part in  $10^{13}$ .

In Table I, we present the atomization energies of the ten rare-gas molecules in the present study. The LDA overbinds these systems by an average of 0.007 eV per atom. For most of the systems the PW91 version of the GGA significantly reduces the overbinding of the LDA. However, the GGA-PW91 functional still results in a significant deviation from experiment. The PBE version of the GGA is in very good agreement with observed atomization energies and has a rms error of 0.0051 eV. In Figs. 1 and 2 we present the binding-

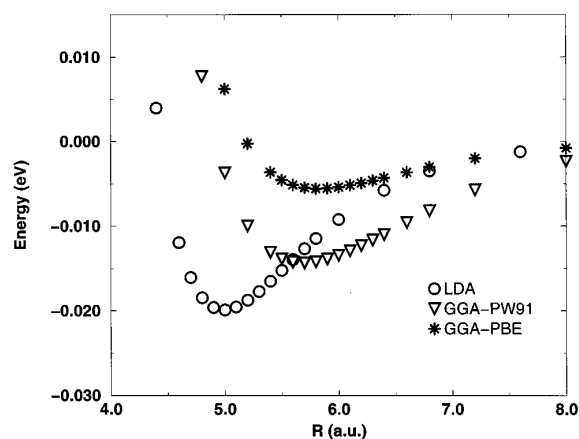


FIG. 2.  $\text{Ne}_2$  binding-energy curves for LDA, GGA-PW91, and GGA-PBE.

energy curves for  $\text{He}_2$  and  $\text{Ne}_2$  as calculated within the three approximations. It is clear that each of these species is bound within the three approximations and that there is a quantitative difference in the two GGA calculations. The most weakly bound dimer,  $\text{He}_2$ , is the most demonstrative of the difference in the GGA functionals with the GGA-PBE providing the most accurate result.  $\text{Ar}_2$ ,  $\text{Kr}_2$ , and  $\text{ArKr}$  are not particularly well described within the GGA-PBE functional. For these dimers the binding energies are calculated to be about half of the experimental binding energy.

Within the PBE version of the GGA, we have calculated the BSSE for  $\text{He}_2$ ,  $\text{Ne}_2$ , and  $\text{Ar}_2$  at their equilibrium bond lengths. The BSSE was found to have increased the binding energy by 0.9%, 2.3%, and 2.4% respectively. Thus the BSSE is not a contributing factor to the binding of these molecules.

Although the basis sets described above are quite extensive, we have investigated the dependence on bases of atomization energies for several of these molecules. For the argon dimer, we have repeated the calculation of the atomization energy at the equilibrium bond length with a basis of all single Gaussians utilizing the same Gaussians as in our basis set discussed previously. Within the PBE version of the GGA, this very extensive basis,  $17s17p17d$ , leads to an atomization energy of 0.006 196 eV with a BSSE of 0.000 167 eV. Thus the difference is only 0.000 096 eV lower than that given in Table I for the argon dimer. In addition, calculations are presented of the homonuclear dimers with minimal basis sets of the  $1s$  function for helium; of  $1s$ ,  $2s$ , and  $2p$  functions for neon; of  $1s$ ,  $2s$ ,  $3s$ ,  $2p$ , and  $3p$  functions for argon; and of  $1s$ ,  $2s$ ,  $3s$ ,  $4s$ ,  $2p$ ,  $3p$ ,  $4p$ , and  $3d$  functions for krypton. This resulted in an atomization energy of 0.0032 eV for  $\text{He}_2$ , 0.0049 eV for  $\text{Ne}_2$ , 0.0049 eV for  $\text{Ar}_2$ , and 0.0049 eV for  $\text{Kr}_2$ .

In Table II, we compare the equilibrium bond lengths calculated within the three approximations to experiment. It is clear for these weakly bound dimers that the LDA leads to bond lengths that grossly underestimate the experimental bond length. The average absolute error compared to experiment for these systems is 0.85 a.u. within the LDA. On the other hand, the two GGA functionals lead to improved agreement with experiment for all the molecules studied. When the  $\text{He}_2$  dimer was studied with a minimal basis, the

equilibrium bond length was found to be 4.24 a.u. for the GGA-PBE functional. With minimal bases, the value for  $\text{Ne}_2$  was 5.87 a.u., for  $\text{Ar}_2$  it was 7.73 a.u., and for  $\text{Kr}_2$  it was 8.49 a.u. The use of an extensive basis of all single Gaussians resulted in a bond length of 7.60 a.u. for  $\text{Ar}_2$ . As was the case for the atomization energies, the bond lengths for  $\text{Ar}_2$ ,  $\text{Kr}_2$ , and  $\text{ArKr}$  do not agree well with experiment for GGA-PBE. However, the GGA-PW91 functional also does an incomplete job of describing the bonding of the three heaviest systems.

In Table III, we present the vibrational modes calculated within the three approximations and the experimental values. Both the calculated harmonic and anharmonic frequencies are listed. The methods used to calculate these frequencies are discussed elsewhere [14]. The modes were calculated using the total energies of at least 30 geometries. As has been previously shown for other molecules [14], the general trend is for the GGA to soften most vibrational modes in comparison with the LDA. For every dimer in this study the GGA-PBE gives a frequency that is lower than that given by the GGA-PW91. Agreement with experiment is best for the GGA-PW91 functional.

We have reported the atomization energies, bond lengths, and vibrational energies for ten rare-gas dimers within the LDA, GGA-PW91, and GGA-PBE approximations to density-functional theory. The results presented include all effects due to self-consistency and basis sets. As anticipated the GGA functionals significantly improve the LDA values for all the molecules in this study. The binding and the vibrational modes are in good agreement with experiment for both the GGA functionals. The PBE version of the GGA results provides a less accurate description for diatomic molecules containing the argon and krypton nuclear species than for those containing helium and neon.

We have also performed these calculations with a minimal basis set. The use of a minimal basis set leads to overlap densities that differ from the overlapping atomic densities by a term that is linear in the overlap of functions on different sites. As such, based on earlier results of Gordon and Kim [1], it would be reasonable to expect an attractive interaction from at least some of the exchange-correlation energy functionals. For all of the homonuclear dimers, we find that the PBE GGA functional leads to bound dimers with a minimal

TABLE II. Equilibrium bond lengths for ten diatomic noble-gas molecules as calculated within the PW91 LDA, PW91 GGA, and PBE GGA. At the bottom of the table are listed in bohrs the average error ( $\delta$ ) and rms error for each of the approximations. Exact values are from Ogilvie and Wang [22].

Molecule	Exact	LDA	GGA-PW91	GGA-PBE
$\text{He}_2$	5.61	4.53	5.00	5.23
$\text{Ne}_2$	5.84	4.99	5.68	5.83
$\text{Ar}_2$	7.10	6.46	7.48	7.61
$\text{Kr}_2$	7.57	7.02	8.10	8.23
$\text{HeNe}$	5.73	4.71	5.33	5.58
$\text{HeAr}$	6.58	5.57	6.28	6.40
$\text{HeKr}$	6.98	5.92	6.70	6.91
$\text{NeAr}$	6.59	5.74	6.54	6.60
$\text{NeKr}$	6.84	6.03	6.86	6.93
$\text{ArKr}$	7.33	6.75	7.91	8.04
$\delta$		-0.845	-0.029	0.119
rms		0.866	0.386	0.376

TABLE III. Harmonic vibrational frequencies in  $\text{cm}^{-1}$  as calculated within the PW91 LDA, PW91 GGA, and PBE GGA. Anharmonic values are given in parentheses. Listed at the bottom of the table are the average error ( $\delta$ ) and rms error in a.u. for each of the approximations. Exact values are from Ogilvie and Wang [22].

Molecule	Exact	LDA	GGA-PW91	GGA-PBE
He <sub>2</sub>		19.17(17.46)	16.80(15.31)	12.27(9.42)
Ne <sub>2</sub>	(13.70)	29.26(26.21)	19.78(16.80)	15.39(10.95)
Ar <sub>2</sub>	(25.74)	28.51(26.25)	12.72(12.59)	10.83(9.89)
Kr <sub>2</sub>	(21.18)	28.18(26.60)	12.49(12.22)	10.97(5.48)
HeNe		25.25(22.49)	16.69(15.27)	11.92(9.97)
HeAr	(5.76)	22.09(19.84)	14.17(13.29)	10.44(8.88)
HeKr	(6.81)	18.87(17.66)	13.96(12.88)	9.62(8.69)
NeAr	(19.10)	28.39(26.08)	15.73(15.01)	12.59(10.90)
NeKr	(18.38)	25.23(24.02)	14.91(14.41)	12.29(10.85)
ArKr	(24.11)	27.45(26.28)	13.23(12.96)	10.39()
$\delta$		(8.00)	(-1.92)	(-6.43)
rms		(9.12)	(7.45)	(9.58)

basis set. The resulting bond lengths are in agreement with those of the full basis-set results by 3%. The resulting binding energies agree within 25% of one another. This suggests that the lowest-order binding is indeed due to the functional form of the density-functional approximation and that it is not due to a redistribution of charge.

Since no mean-field treatment is capable of reproducing the long-range fluctuating dipole ( $1/r^6$ ) attraction between closed-shell systems, and since it is unclear whether this mechanism should be the primary bonding mechanism in rare-gas systems, we have also examined the contribution to the binding due to the van der Waals forces at both the experimental bond length and the predicted GGA-PBE bond lengths given in Table II. This energy is referred to as the dispersion energy and is approximated by  $u(r) = -(3\alpha_1\alpha_2/2r^6)(I_1I_2/I_1+I_2)$ , where  $\alpha_i$  is the polarizability of the  $i$ th atom and  $I_i$  is the ionization potential of the  $i$ th atom [16]. For the case of dimers of like nuclear species this expression becomes  $u(r) = -(3\alpha^2/4r^6)I$ . The

TABLE IV. Dispersion energy in eV due to van der Waals attractive forces at the experimental and GGA-PBE bond distances. The polarizabilities and ionization potentials used to calculate these dispersion energies were from GGA-PBE atomic calculations.

Molecule	Exact $r_e$	GGA-PBE $r_e$
He <sub>2</sub>	0.000 85	0.001 30
Ne <sub>2</sub>	0.002 87	0.002 90
Ar <sub>2</sub>	0.009 59	0.006 32
Kr <sub>2</sub>	0.013 06	0.007 91
HeNe	0.001 55	0.001 82
HeAr	0.002 18	0.002 57
HeKr	0.002 13	0.002 26
NeAr	0.004 51	0.004 46
NeKr	0.005 04	0.004 66
ArKr	0.011 18	0.006 42

dispersion energies for dimers of like and unlike nuclear species are given in Table IV at bond lengths corresponding to the experimental and GGA-PBE values. In all cases we find that the net dispersion energy is smaller than the experimental binding energy. Since there will clearly be some kinetic-energy-induced repulsion at the experimental bond lengths, we suggest that an additional short-ranged overlap-induced attraction is indeed necessary to obtain quantitative agreement with experiment. Further, for the heavier atoms it appears that the agreement between experiment and theory could be improved if a mechanism which allowed for both short-range overlap attractions and long-range dispersion attractions could be identified.

We thank Dr. D.V. Porezag for generating fully optimized Gaussian basis sets for these studies. We thank Dr. J. P. Perdew, Dr. K. Burke, and Dr. M. Ernzerhof for providing us with subroutines for their simplified GGA method. Work was supported in part by the ONR Georgia Tech Molecular Design Institute (N00014-95-1-1116) and the NSF (DAAD INT-9514714). D.C.P. acknowledges the support of the National Research Council. M.R.P. acknowledges computational support from the Department of Defense High Performance Computing Centers.

- [1] R. G. Gordon and Y. S. Kim, *J. Chem. Phys.* **56**, 3122 (1972).  
 [2] R. G. Parr and W. Yang in *Density-Functional Theory of Atoms and Molecules* (Oxford University Press, Oxford, England, 1989), p. 219.  
 [3] P. Hohenberg and W. Kohn, *Phys. Rev. B* **136**, 864 (1964); W. Kohn and L. J. Sham, *Phys. Rev.* **140**, A1133 (1965).  
 [4] J. P. Worth *et al.* *Chem. Phys. Lett.* **55**, 168 (1978).  
 [5] D. J. Lacks and R. G. Gordon, *Phys. Rev. A* **47**, 4681 (1993).  
 [6] J. P. Perdew and Y. Wang, *Phys. Rev. B* **33**, 8800 (1986).  
 [7] A. D. Becke, *J. Chem. Phys.* **84**, 4524 (1986); **85**, 7184 (1986); *Phys. Rev. A* **38**, 3098 (1988).  
 [8] A. E. DePristo and J. D. Kress, *J. Chem. Phys.* **86**, 1425 (1987).  
 [9] J. P. Perdew *et al.* *Phys. Rev. B* **46**, 6671 (1992); **48**, 4979(E) (1993).  
 [10] J. M. Perez-Jorda and A. D. Becke, *Chem. Phys. Lett.* **233**, 134 (1995).  
 [11] A. D. Becke, *J. Chem. Phys.* **98**, 1372 (1993).  
 [12] A. D. Becke, *J. Chem. Phys.* **98**, 5648 (1993).  
 [13] J. P. Perdew and Y. Wang, *Phys. Rev. B* **45**, 13 244 (1992).  
 [14] D. C. Patton *et al.* *Phys. Rev. B* **55**, 7454 (1997).  
 [15] J. F. Dobson and B. P. Dinte, *Phys. Rev. Lett.* **76**, 1780 (1996).  
 [16] F. London, *Z. Phys. Chem. Abt. B* **11**, 222 (1930); *Z. Phys. Chem. (Munich)* **60**, 491 (1930); *Trans. Faraday Soc.* **33**, 8 (1937).  
 [17] J. P. Perdew *et al.* *Phys. Rev. Lett.* **77**, 3865 (1996).  
 [18] K. A. Jackson and M. R. Pederson, *Phys. Rev. B* **42**, 3276 (1990); M. R. Pederson and K. A. Jackson, *ibid.* **43**, 7312 (1991); in *Density Functional Methods in Chemistry*, edited by J. K. Labanowski and J. W. Andzelm (Springer-Verlag, Berlin, 1991).  
 [19] M. R. Pederson and K. A. Jackson, *Phys. Rev. B* **41**, 7453 (1990).  
 [20] D. V. Porezag, Ph.D. thesis, Chemitz Technical Institute, 1997 (unpublished).  
 [21] S. F. Boys and F. Bernardi, *Mol. Phys.* **19**, 553 (1970).  
 [22] J. F. Ogilvie and F. Y. H. Wang, *J. Mol. Struct.* **273**, 277 (1992); **291**, 313 (1993).